Inorganic Chemistry
Article

Inorg. Chem. **2010**, *49*, 6545–6551 **6545**
DOI: 10.1021/ic100427t

Theoretical Studies of $An^{II}_2(C_8H_8)_2$ (An = Th, Pa, U, and Np) Complexes: The Search for Double-Stuffed Actinide Metallocenes

Jia Zhou, Jason L. Sonnenberg,† and H. Bernhard Schlegel*

Department of Chemistry, Wayne State University, Detroit, Michigan 48202.
†Present Address: Department of Chemistry, Stevenson University, Stevenson, Maryland 21153

Received March 3, 2010

Complexes of the form $An_2(C_8H_8)_2$ (An = Th, Pa, U, and Np) were investigated using density functional theory with scalar-relativistic effective core potentials. For uranium, a coaxial isomer with D_{8h} symmetry is found to be more stable than a C_s isomer in which the dimetal unit is perpendicular to the C_8 ring axis. Similar coaxial structures are predicted for $Pa_2(C_8H_8)_2$ and $Np_2(C_8H_8)_2$, while in $Th_2(C_8H_8)_2$, the C_8H_8 rings tilt away from the An−An axis. Going from $Th_2(C_8H_8)_2$ to $Np_2(C_8H_8)_2$, the An−An bond length decreases from 2.81 Å to 2.19 Å and the An−An stretching frequency increases from 249 to 354 cm^{-1}. This is a result of electrons populating An−An 5f π- and δ-type bonding orbitals and ϕ nonbonding orbitals, thereby increasing in An−An bond order. $U_2(C_8H_8)_2$ is stable with respect to dissociation into $U(C_8H_8)$ monomers. Disproportionation of $U_2(C_8H_8)_2$ into uranocene and the U atom is endothermic but is slightly exothermic for uranocene plus $^1/_2U_2$, suggesting that it might be possible to prepare double stuffed uranocene if suitable conditions can be found to avoid disproportionation.

1. Introduction

The subject of metal−metal multiple bonds has received a great deal of attention from both experimentalists and theoreticians since Cotton et al.'s 1964 discovery of the δ bond in $[Re_2Cl_8]^{2-}$.[1] Although metal−metal multiple bonds abound in the transition metals,[2,3] molecules containing unambiguous actinide−actinide bonds are limited. In 1974, a uranium dimer, U_2, and U_2O_2 were detected in the gas phase via mass spectrometry but were not isolated.[4] More recently, Andrews et al. have detected, but not crystallized, $U^I(\mu\text{-}H)_2U^I$ in both solid Ar and Ne.[5,6] Progress has been made in preparing and structurally characterizing U−M bonds for main group metals.[7−10] However, creating an isolatable molecule containing actinide−actinide bonds that can be crystallized is still a cutting edge problem requiring synergistic efforts between experimentation and theory.

Bursten and co-workers were the first to theoretically investigate U_2 and found that six of the 12 valence electrons occupy the $7s\sigma_g$ and $6d\pi_u$ orbitals.[11−13] Gagliardi and Roos confirmed these results with state of the art calculations and predicted that U_2 forms a quintuple bond with a dissociation energy of 127 kJ/mol.[14] Roos and co-workers expanded their investigation and showed that Ac_2, Th_2, and Pa_2 will form double, quadruple, and quintuple bonds, respectively.[15] They also predicted that $[U_2]^{2+}$ is a metastable species with a triple bond that could be stabilized by complexation with chloride, carboxylate, or phenyl ligands.[16−18] Kaltsoyannis and Cavigliasso studied the series M_2X_6 (M = U, W, Mo; X = Cl, F,

*To whom correspondence should be addressed. Tel.: (313) 577-2562. Fax: (313) 577-8822. E-mail: hbs@chem.wayne.edu.

(1) Cotton, F. A.; Curtis, N. F.; Harris, C. B.; Johnson, B. F. G.; Lippard, S. J.; Mague, J. T.; Robinson, W. R. *Science* **1964**, *145*, 1305–1307.
(2) Chisholm, M. H.; Macintosh, A. M. *Chem. Rev.* **2005**, *105*, 2949–2976.
(3) Cotton, F. A.; Murillo, C. A.; Walton, R. A. *Multiple Bonds between Metal Atoms*, 3rd ed.; Springer Science and Business Media, Inc.: New York, 2005; p 856.
(4) Gorokhov, L. N.; Emel'yanov, A. M.; Khodeev, Y. S. *Teplofiz. Vys. Temp.* **1974**, *12*, 1307–1309.
(5) Souter, P. F.; Kushto, G. P.; Andrews, L.; Neurock, M. *J. Am. Chem. Soc.* **1997**, *119*, 1682–1687.
(6) Raab, J.; Lindh, R. H.; Wang, X.; Andrews, L.; Gagliardi, L. *J. Phys. Chem. A* **2007**, *111*, 6383–6387.
(7) Porchia, M.; Casellato, U.; Ossola, F.; Rossetto, G.; Zanella, P.; Graziani, R. *J. Chem. Soc., Chem. Commun.* **1986**, 1034–1035.
(8) Minasian, S. G.; Krinsky, J. L.; Williams, V. A.; Arnold, J. *J. Am. Chem. Soc.* **2008**, *130*, 10086.
(9) Minasian, S. G.; Krinsky, J. L.; Rinehart, J. D.; Copping, R.; Tyliszczak, T.; Janousch, M.; Shuh, D. K.; Arnold, J. *J. Am. Chem. Soc.* **2009**, *131*, 13767–13783.
(10) Liddle, S. T.; McMaster, J.; Mills, D. P.; Blake, A. J.; Jones, C.; Woodul, W. D. *Angew. Chem., Int. Ed.* **2009**, *48*, 1077–1080.
(11) Bursten, B. E.; Ozin, G. A. *Inorg. Chem.* **1984**, *23*, 2910–2911.
(12) Pepper, M.; Bursten, B. E. *J. Am. Chem. Soc.* **1990**, *112*, 7803–7804.
(13) Kaltsoyannis, N.; Hay, P. J.; Li, J.; Blaudeau, J.-P.; Bursten, B. E. In *The Chemistry of the Actinide and Transactinide Elements*, 3rd ed.; Morss, L. R., Edelstein, N. M., Fuger, J., Eds.; Springer: New York, 2006; Vol. *3*, pp 1893−2012.
(14) Gagliardi, L.; Roos, B. O. *Nature* **2005**, *433*, 848–851.
(15) Roos, B. O.; Malmqvist, P.-Å.; Gagliardi, L. *J. Am. Chem. Soc.* **2006**, *128*, 17000–17006.
(16) Gagliardi, L.; Pyykkö, P.; Roos, B. O. *Phys. Chem. Chem. Phys.* **2005**, *7*, 2415–2417.
(17) Roos, B. O.; Gagliardi, L. *Inorg. Chem.* **2006**, *45*, 803–807.
(18) La Macchia, G.; Brynda, M.; Gagliardi, L. *Angew. Chem., Int. Ed.* **2006**, *45*, 6210–6213.

Published on Web 06/14/2010

OH, NH_2, CH_3) and $[M_2X_8]^{2-}$ (M = U, Np, Pu, Mo, Tc, Ru, W, Re, Os; X = Cl, Br, I) with density functional and multiconfigurational methods and found that multiple metal−metal bonds exist in all species.[19,20] Straka and Pyykkö demonstrated that HTh^ITh^IH is linear, unlike $U^I(\mu\text{-}H)_2U^I$,[5] and has a Th−Th triple bond.[21] They point out that HTh^I-Th^IH may already have been seen in a solid Ar matrix and that it is stabilized by ligands other than hydrogen.[21] Wu and Lu have calculated $U_2@C_{60}$, showing that U_2 forms multiple bonds when encased endohedrally in a small fullerene.[22] However, for larger fullerenes such as C_{70} and C_{84}, Infante and co-workers have demonstrated that the U−U bond no longer exists because the individual atoms bind preferentially to the inner walls of the fullerenes.[23] The binding of actinides in smaller organometallic complexes is somewhat different. Infante et al. predicted that $An_2(C_6H_6)_2$ complexes will be more stable than two isolated MC_6H_6 monomers for M = Th and U.[24] In spite of all these theoretical efforts, the best ligand set for stabilizing actinide−actinide multiple bonds is still elusive, but recent experimental advances are hinting at new alternatives.

The discovery of $Zn^I_2(\eta^5\text{-}C_5Me_5)_2$ and its derivatives has fundamentally changed the definition of metallocene by introducing bimetallic units to the center of the classic sandwich complex.[25−27] Although no other dimetallocenes are experimentally known so far, a plethora of theoretical work has predicted that such molecules should exist for a variety of alkaline earth and transition metals.[26−42] Dimetallocenes may also exist for systems with rings that are not composed of carbon, such as hydrosilver, phosphorus, boron, and nitrogen.[43−46] Along with other recently synthesized LM^IM^IL compounds, M = Cr[47] and Mg,[48] these molecules demonstrate how this bonding motif can stabilize unusual, low-oxidation states of metals. Since metallocenes with D_{8h} symmetry employing COT (COT = $[C_8H_8]^{2-}$) rings have been synthesized for thorium, protactinium, uranium, neptunium, and plutonium,[49] actinide (An) dimers may be stabilized by two COT rings in a similar manner to LM^IM^IL compounds, thereby forming new dimetallocene complexes that might be isolatable. In this work, density functional theory (DFT) methods are employed to study the possible sandwich compounds of $An_2(COT)_2$ (An = Th, Pa, U, Np). To the best of our knowledge, there is no other earlier work on this aspect.

2. Computational Methodology

All computations employed the hybrid B3LYP functional[50−52] and were carried out using the development version of Gaussian.[53] For the actinide atoms, scalar relativistic effects were taken into account via the relativistic effective core potential (RECP) of Küchle et al.[54] This RECP places 60 electrons in the actinide core leaving the 5s, 5p, 5d, 6s, 6p, 5f, 6d, and 7s electrons for explicit treatment. The most diffuse s, p, d, and f Gaussian functions of the associated actinide basis set were removed to generate the [7s 6p 5d 3f] basis that previously predicted accurate molecular structures.[55,56] Ligand atoms were described with Dunning's cc-pVDZ basis set.[57] Pure d and f functions were used in all Gaussian basis sets. Harmonic vibrational frequencies were computed to confirm that each structure was a local minimum on the potential energy surface and to provide zero-point energy corrections. An integration grid with 400 radial shells and 770 angular points per shell was employed for all DFT calculations. The stability of each structure's density was tested using standard methods[58] and reoptimized if necessary. Natural population analysis[59] (NPA) was performed on each structure using a valence space composed of 5f, 6d, 7s, and 7p.[60,61] GaussView was used to create all structure and molecular orbital pictures.[62] For diuranocene, calculations employing a frozen-core approximation[63] and the zero-order regular approximation[64−66] (ZORA) Hamiltonian to account for scalar relativistic effects were also run with the ADF code.[67]

(19) Kaltsoyannis, N.; Cavigliasso, G. *Dalton Trans*. **2006**, 5476–5483.
(20) Kaltsoyannis, N.; Cavigliasso, G. *Inorg. Chem*. **2006**, *45*, 6828–6839.
(21) Straka, M.; Pyykkö, P. *J. Am. Chem. Soc*. **2005**, *127*, 13090–13091.
(22) Wu, X.; Lu, X. *J. Am. Chem. Soc*. **2007**, *129*, 2171–2177.
(23) Infante, I.; Gagliardi, L.; Scuseria, G. E. *J. Am. Chem. Soc*. **2008**, *130*, 7459–7465.
(24) Infante, I.; Raab, J.; Lyon, J. T.; Liang, B.; Andrews, L.; Gagliardi, L. *J. Phys. Chem. A* **2007**, *111*, 11996–12000.
(25) Resa, I.; Carmona, E.; Gutierrez-Puebla, E.; Monge, A. *Science* **2004**, *305*, 1136–1138.
(26) del Rio, D.; Galindo, A.; Resa, I.; Carmona, E. *Angew. Chem., Int. Ed*. **2005**, *44*, 1244–1247.
(27) Grirrane, A.; Resa, I.; Rodriguez, A.; Carmona, E.; Alvarez, E.; Gutierrez-Puebla, E.; Monge, A.; Galindo, A.; del Rio, D.; Andersen, R. A. *J. Am. Chem. Soc*. **2007**, *129*, 693–703.
(28) Xie, Y. M.; Schaefer, H. F.; King, R. B. *J. Am. Chem. Soc*. **2005**, *127*, 2818–2819.
(29) Pandey, K. K. *J. Organomet. Chem*. **2007**, *692*, 1058–1063.
(30) Kan, Y. H. *THEOCHEM* **2007**, *805*, 127–132.
(31) Zhou, J.; Wang, W. N.; Fan, K. N. *Chem. Phys. Lett*. **2006**, *424*, 247–251.
(32) Liu, Z. Z.; Tian, W. Q.; Feng, J. K.; Zhang, G.; Li, W. Q. *THEOCHEM* **2006**, *758*, 127–138.
(33) Kress, J. W. *J. Phys. Chem. A* **2005**, *109*, 7757–7763.
(34) Xie, Z. Z.; Fang, W. H. *Chem. Phys. Lett*. **2005**, *404*, 212–216.
(35) Philpott, M. R.; Kawazoe, Y. *THEOCHEM* **2006**, *776*, 113–123.
(36) Philpott, M. R.; Kawazoe, Y. *THEOCHEM* **2006**, *773*, 43–52.
(37) Philpott, M. R.; Kawazoe, Y. *Chem. Phys*. **2006**, *327*, 283–290.
(38) Philpott, M. R.; Kawazoe, Y. *Mater. Trans*. **2007**, *48*, 693–699.
(39) Philpott, M. R.; Kawazoe, Y. *Chem. Phys*. **2007**, *333*, 201–207.
(40) Kua, J.; Tomlin, K. M. *J. Phys. Chem. A* **2006**, *110*, 11988–11994.
(41) Wang, H. M.; Yang, C. L.; Wan, B. S.; Han, K. L. *J. Theory Comput. Chem*. **2006**, *5*, 461–473.
(42) Xu, B.; Li, Q. S.; Xie, Y.; King, R. B.; Schaefer, H. F. *J. Chem. Theory Comput*. **2010**, *6*, 735–746.
(43) Zhou, J.; Xiao, F.; Liu, Z. P.; Fan, K. N. *THEOCHEM* **2007**, *808*, 163–166.
(44) Liu, Z. Z.; Tian, W. Q.; Feng, J. K.; Li, W. Q.; Cui, Y. H. *THEOCHEM* **2007**, *809*, 171–179.
(45) Li, Q. S.; Xu, Y. *J. Phys. Chem. A* **2006**, *110*, 11898–11902.
(46) Zhang, X. H.; Li, S.; Li, Q. S. *J. Theory Comput. Chem*. **2006**, *5*, 475–487.
(47) Nguyen, T.; Sutton, A. D.; Brynda, M.; Fettinger, J. C.; Long, G. J.; Power, P. P. *Science* **2005**, *310*, 844–847.
(48) Green, S. P.; Jones, C.; Stasch, A. *Science* **2007**, *318*, 1754–1757.
(49) Seyferth, D. *Organometallics* **2004**, *23*, 3562–3583.
(50) Becke, A. D. *J. Chem. Phys*. **1993**, *98*, 5648–5652.
(51) Lee, C.; Yang, W.; Parr, R. D. *Phys. Rev. B* **1988**, *37*, 785–789.
(52) Stephens, P. J.; Devlin, F. J.; Chabalowski, C. F.; Frisch, M. J. *J. Phys. Chem*. **1994**, *98*, 11623–11627.
(53) Frisch, M. J.; Trucks, G. W.; Schlegel, H. B.; Scuseria, G. E. *Gaussian DV*, revision F.02; Gaussian, Inc.: Wallingford, CT, 2007.
(54) Küchle, W.; Dolg, M.; Stoll, H.; Preuss, H. *J. Chem. Phys*. **1994**, *100*, 7535–7542.
(55) Hratchian, H. P.; Sonnenberg, J. L.; Hay, P. J.; Martin, R. L.; Bursten, B. E.; Schlegel, H. B. *J. Phys. Chem. A* **2005**, *109*, 2255–2262.
(56) Sonnenberg, J. L.; Hay, P. J.; Martin, R. L.; Bursten, B. E. *Inorg. Chem*. **2005**, 2255–2262.
(57) Dunning, T. H. *J. Chem. Phys*. **1989**, *90*, 1007–1023.
(58) Seeger, R.; Pople, J. A. *J. Chem. Phys*. **1977**, *66*, 3045–3050.
(59) Glendening, E. D.; Badenhoop, J. K.; Reed, A. E.; Carpenter, J. E.; Bohmann, J. A.; Morales, C. M. *NBO 5.0*; Theoretical Chemistry Institute, University of Wisconsin: Madison, WI, 2001.
(60) Clark, A. E.; Sonnenberg, J. L.; Hay, P. J.; Martin, R. L. *J. Chem. Phys*. **2004**, *121*, 2563–2570.
(61) Maseras, F.; Morokuma, K. *Chem. Phys. Lett*. **1992**, *195*, 500–504.
(62) Dennington, R., II; Keith, T.; Millam, J. M.; Eppinnett, K.; Hovell, W. L.; Gilliland, R. *GaussView*, 3.09; Semichem, Inc.: Shawnee Mission, KS, 2003.
(63) Baerends, E. J.; Ellis, D. E.; Ros, P. *Chem. Phys*. **1973**, *2*, 41–51.
(64) Lenthe, E. v.; Baerends, E. J.; Snijders, J. G. *J. Chem. Phys*. **1993**, *99*, 4597–4610.

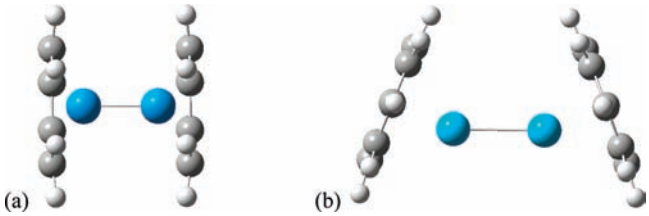

Figure 1. Optimized structures of (a) D_{8h} $An_2(COT)_2$ (An = Pa, U, and Np) and (b) C_{2v} $Th_2(COT)_2$ with C and H atoms denoted in black and white, respectively.

The BLYP[50,51] functional and a TZ2P ligand basis set along with a TZP uranium basis set were used for the ZORA calculations.

3. Results and Discussion

The formation of an actinocene, $An^{IV}(COT)_2$, is a well-known thermodynamic sink on the An plus COT potential energy surface. If the disproportionation channel converting $An^{II}_2(COT)_2$ to $An^{IV}(COT)_2$ can be cleverly disabled, then a rich field of actinide dimetallocene chemistry becomes accessible (*vide infra*). Because the uranium dimer has received more attention than other early An dimers, the discussion starts with $U_2(COT)_2$. Since proceeding to neptunium and beyond in the periodic table places electrons in nonbonding 5f φ orbitals, the maximum An−An bond order should be achieved in $U_2(COT)_2$ or $Np_2(COT)_2$. This is counterbalanced by contraction of the 5f orbitals with increasing atomic number, which diminishes the bond strength. On the basis of the energetics of $U_2(COT)_2$ isomers, only coaxial structures for protactinium, neptunium, and thorium are presented. The energy difference between the D_{8d} and D_{8h} coaxial conformers is very small ($\Delta G(0\,K) = 0.071$ kJ/mol for Pa) as expected on the basis of the actinocene crystal structures,[68−73] so only D_{8h} coaxial species were investigated. The thorium complex is unusual in comparison to the other early actinides and so is described last.

3.1. Uranium. On the basis of Gagliardi's work,[11,14] we expect the U_2 complexes to be stable. A coaxial arrangement, where the uranium atoms lie along the C_8 rotational axis of the COT rings, leads to a $^3A_{1g}$ predicted ground state (see Figure 1) with D_{8h} symmetry. The value of $<S^2>$ is 2.024, and orbital stability analysis indicates that the triplet wave function is stable (the quintet state is 63 kJ/mol higher). The U−U bond length of 2.240 Å (Table 1) is at least a U−U triple bond, on the basis of a U triple-bond covalent radius of 1.18 Å.[74] This bond length agrees rather well with the ZORA-BLYP result of 2.285 Å. With a U to ring centroid distance only 0.065 Å longer than in the crystal structure of uranocene,[70] and 0.021 Å longer than in uranocene (1.968 Å) at the same level of theory, $U_2(\eta^8\text{-COT})_2$ can be accurately described as a dimer of two UCOT half-sandwich complexes. The COT ring remains almost the same in diuranocene compared to that in uranocene: the C−C bond is 1.415 Å in diuranocene while the C−C bonds are 1.416 Å in uranocene, and the C−H bond is 1.093 Å in both diuranocene and uranocene. Furthermore, the U−C distance is 2.715 Å in diuranocene, while it is only 0.015 Å shorter in uranocene. $U_2(COT)_2$ can be described equally well as $[U_2]^{4+}$ complexed with two COT ligands. The U−U bond in $U_2(COT)_2$ (2.240 Å) is nearly the same as in $[U_2]^{4+}$ (2.297 Å). This indicates that the strength of the U−U bond originates from the stability of $[U_2]^{4+}$ and not from its interactions with the COT ligands.

Each UCOT monomer has four U valence electrons available for metal−metal bonding. The quintet state is the most stable and has one electron in an s plus f σ-type orbital and two unpaired electrons in the f π-type orbitals and one electron in an f ϕ-type orbital (see Figure 2). Under C_{8v} symmetry, these orbitals are $1a_1$, $1e_1$, and $1e_3$, respectively. When two UCOT monomers are brought together to form a $U_2(COT)_2$ dimer, these eight U f electrons occupy five bonding molecular orbitals (MOs) for an electron configuration of $\sigma^2\pi^4\delta^2$ and a formal U−U bond order of 4. Natural population analysis yields a Wiberg bond order of 4.3 for this interaction. The U−U bonding MOs are shown in Figure 3, and it is interesting to compare them to those previously reported for U_2[11,14] and $[U_2]^{2+}$.[16] The $1a_{1g}$ MO is the U−U σ bond formed from the in-phase mixing of the UCOT $1a_1$ group orbitals. This same MO is seen in both U_2 and $[U_2]^{2+}$ where the authors' orbital assignment indicates that the 7s contribution was perceived to be larger than the $5f_\sigma$ contribution.[14,16] The $1e_{1u}$ orbital in U_2COT_2 is a π-type metal−metal bonding MO formed from U $5f_\pi$ atomic orbitals. This U−U bonding MO was also found in U_2, $[U_2]^{2+}$, and diuranium tetraformate; since the 6d contribution appeared to be larger than the $5f_\pi$, the orbital was designated $6d_\pi$.[16,17] It should be noted that MO pictures can be deceiving. For example, Figure 4 shows that the choice of isovalue can artificially suggest a larger s contribution than is borne out by the Mulliken percent character analysis (see Table 2). As indicated by the Mulliken percent character, the $1\sigma_g$ orbitals of $[U_2]^{4+}$ and the $1a_{1g}$ orbital in U_2COT_2 are better described as $5f_\sigma$; likewise, the $1\pi_u$ and $1e_{1u}$ orbitals should be designated $5f_\pi$. The $1e_{2g}$ MO is the U−U δ bond formed from the in-phase combination of $5f_\delta$ atomic orbitals and is also present in U_2 and $[U_2]^{2+}$. The gerade and ungerade combinations of the formally nonbonding U $5f_\varphi$ orbitals lead to the $1e_{3u}$ and $1e_{3g}$ MOs that are also seen in U_2 and $[U_2]^{2+}$. Although spin−orbit coupling should not significantly affect molecular geometries,[75] it will remove the degeneracy of the e_{iu} and e_{ig}, $i = 1-3$, MOs. Depending upon the energy difference between the $e_{3/2g}$ and $e_{5/2g}$ D_{8h}* double-group MOs resulting from the single-group

(65) Lenthe, E. v.; Baerends, E. J.; Snijders, J. G. *J. Chem. Phys.* **1994**, *101*, 9783–9792.
(66) Lenthe, E. v.; Ehlers, A.; Baerends, E. J. *J. Chem. Phys.* **1999**, *110*, 8943–8953.
(67) Baerends, E. J. et al. *ADF2007.01*; SCM, Theoretical Chemistry, Vrije Universiteit: Amsterdam, The Netherlands. http://www.scm.com (accessed Jun 2010).
(68) Streitwieser, A.; Mueller-Westerhoff, U. *J. Am. Chem. Soc.* **1968**, *90*, 7364–7364.
(69) Zalkin, A.; Raymond, K. N. *J. Am. Chem. Soc.* **1969**, *91*, 5667–5668.
(70) Avdeef, A.; Raymond, K. N.; Hodgson, K. O.; Zalkin, A. *Inorg. Chem.* **1972**, *11*, 1083–1088.
(71) Streitwieser, A.; Yoshida, N. *J. Am. Chem. Soc.* **1969**, *91*, 7528–7528.
(72) Karraker, D. G.; Stone, J. A.; Jones, E. R.; Edelstein, N. *J. Am. Chem. Soc.* **1970**, *92*, 4841–4845.
(73) Starks, D. F.; Parsons, T. C.; Streitwieser, A.; Edelstein, N. *Inorg. Chem.* **1974**, *13*, 1307–1308.
(74) Pyykkö, P.; Riedel, S.; Patzschke, M. *Chem.—Eur. J.* **2005**, *11*, 3511–3520.
(75) Li, J.; Bursten, B. E. In *Computational Organometallic Chemistry*; Cundari, T. R., Ed.; Dekker: New York, 2001; pp 345−379.

Table 1. Calculated Gas-Phase Bond Lengths (Å), Bond Angles (deg), Natural Charges (e), and Vibrational Frequencies (cm^{-1}) for $An_2(COT)_2$ Complexes with Vibrational Mode Symmetries in Parentheses

An	symmetry	An−An	An−X[a]	HCX[a]	AnAnX[a]	An natural charge	An−An ν_{sym}
Th	C_{2v} $^3B_1$	2.809	2.029	5.4	158.4	0.86	249 (A_1)
Pa	D_{8h} $^5A_{1g}$	2.537	1.998	4.8	180.0	0.93	270 (A_{1g})
U	D_{8h} $^3A_{1g}$	2.240	1.989	5.7	180.0	0.77	349 (A_{1g})
Np	D_{8h} $^5A_{1g}$	2.189	1.938	5.8	180.0	0.80	354 (A_{1g})

[a] X is the centroid of the COT ring.

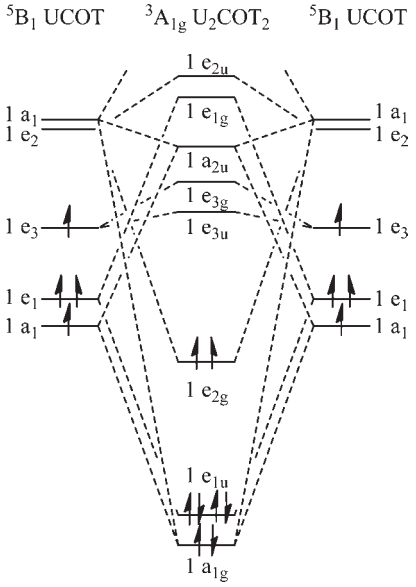

Figure 2. Qualitative canonical MO diagram showing the interaction of two $^5B_1$ UCOT monomers under single-group C_{8v} symmetry to form $^3A_{1g}$ $U_2(\eta^8\text{-COT})_2$ under single-group D_{8h} symmetry. Only the U 5f electron manifold of U_2COT_2 is shown for clarity (see text). Orbital energies are taken as the average of the α and β components. Since the UCOT density breaks symmetry, the closest C_{8v} symmetry labels are used.

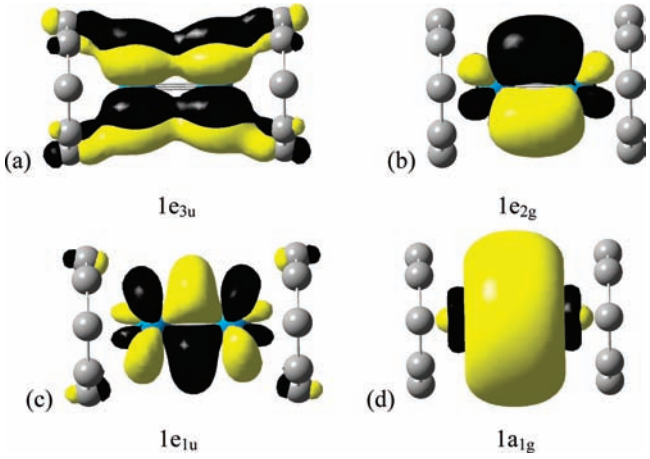

Figure 3. Selected D_{8h} $U_2(COT)_2$ α molecular orbitals (a) LUMO, (b) HOMO−1, and (d) HOMO−2 plotted at an isovalue of 0.02. Hydrogens were omitted for clarity.

$1e_{2g}$ MO, the ground state may be singlet, but this is not expected on the basis of the high-spin nature of free U_2.[14]

On the basis of the work of Xie et al.[28] on Ni_2Cp_2 and Cu_2Cp_2 in which metal−metal bonds prefer to be perpendicular to the C_5 axis of the Cp rings and the work of Infante et al.[24] on $U_2(C_6H_6)_2$ and $Th_2(C_6H_6)_2$ where the

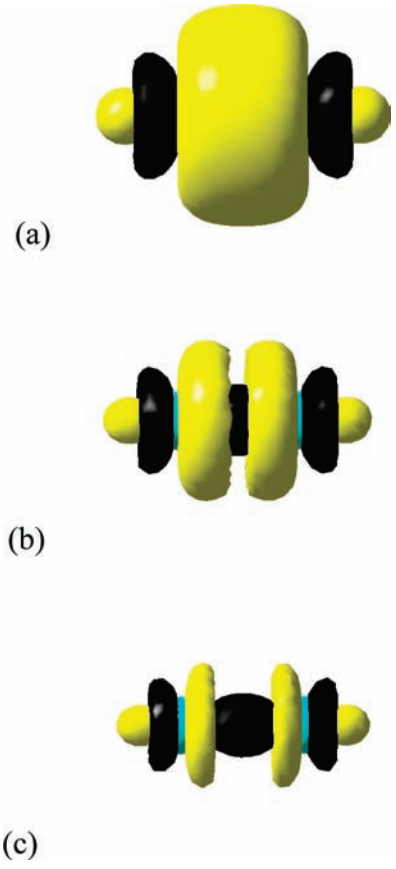

Figure 4. $1\sigma_g$ MO for triplet $[U_2]^{4+}$ plotted at an isovalue of (a) 0.02, (b) 0.04, and (c) 0.06.

An−An bonds are approximately perpendicular to the C_6 axis of the benzene rings, a second isomer of $U_2(COT)_2$ with the U−U bond perpendicular to the C_8 axis of the rings was also considered. Rotation of the U_2 unit in D_{8h} $U_2(\eta^8\text{-COT})_2$ by 90° generates a D_{2h} fifth-order saddle point (SP) 203 kJ/mol (ΔG(0 K)) higher in energy than the D_{8h} isomer. The COT rings are slightly puckered in the D_{2h} isomer, and the U−U bond has lengthened to 2.368 Å. Reducing the symmetry constraints to C_{2h} produces a lower energy (ΔG(0 K) = 138 kJ/mol), third-order SP in which two of the eight C atoms in each ring bend out of plane by 44° and the U−U bond is 2.811 Å. Further reduction of symmetry constraints increases the out-of-plane bending to 52° and forms a C_s structure 28.0 kJ/mol (ΔG(0 K)) *higher* in energy than the coaxial isomer. This energetic ordering of coaxial diuranocene that is more stable than perpendicular diuranocene is the opposite of Cu and Ni M_2Cp_2 complexes where the perpendicular isomers are predicted to be more stable than the coaxial species. Diuranocene is more like Zn_2Cp_2, for which the

Table 2. Uranium Mulliken % Character for Selected α MOs

MO	s	p	d	f	assignment
		$[U_2]^{4+}$ $D_{\infty h}$ triplet			
$1\pi_u$		1	40	59	$5f_\pi$
$1\sigma_g$	8	3	6	83	$5f_\sigma$
$1\delta_g$			5	95	$5f_\delta$
		$Th^{II}_2(\eta^8\text{-COT})_2$ D_{8h} triplet			
$1a_{1g}$	50	0	24	16	$5f_\sigma$
$1e_{1u}$		4	56	32	$5f_\pi$
$1e_{2g}$			48	48	$5f_\delta$
		$Pa^{II}_2(\eta^8\text{-COT})_2$ D_{8h} quintet			
$1a_{1g}$	34	4	6	56	$5f_\sigma$
$1e_{1u}$			20	76	$5f_\pi$
$1e_{2g}$			20	74	$5f_\delta$
		$U^{II}_2(\eta^8\text{-COT})_2$ D_{8h} triplet			
$1a_{1g}$	34	6	14	46	$5f_\sigma$
$1e_{1u}$			24	70	$5f_\pi$
$1e_{2g}$			24	76	$5f_\delta$
		$Np^{II}_2(\eta^8\text{-COT})_2$ $D_{\infty h}$ quintet			
$1a_{1g}$	24	6	10	60	$5f_\sigma$
$1e_{1u}$			16	80	$5f_\pi$
$1e_{2g}$			22	76	$5f_\delta$

coaxial structure is stable but the perpendicular complex is not a stationary point.[28]

As seen in Figure 5, the COT ring aromaticity is perturbed upon bending, and the rings have slipped from η^8 to μ-η^6,η^4. This reduced hapticity is a slight perturbation of the more common μ-η^5,η^5 interaction seen in $M_2(\mu$-η^5,η^5-COT)R_n (M = Cr, Mo, W; R = COT, $OCH_2{}^tBu$, O^iPr, O^tBu) compounds.[76−78] In these compounds, X-ray crystallography showed that the pair of closely bonded metal atoms lies over one sharply folded COT ring, and each metal atom symmetrically bonds to five carbon atoms of this COT ring. Each metal atom also is attached to the R group. However, in our C_s conformer, each ring can still interact with both metals since six U−C distances are less than 2.72 Å to one of the U atoms and four U−C distances are less than 2.75 Å to the other, compared with 2.715 Å in D_{8h} $U_2(\eta^8\text{-COT})_2$. The COT ligand in the perpendicular species can be compared to similar calculations on the free C_8H_8 ring, aka neutral [8]annulene, which adopts a ground state D_{2d} geometry with alternating carbon single and double bonds of 1.475 and 1.345 Å, respectively, and puckers to a boat-like structure, consistent with experiment values. Thus, the C_8H_8 rings in the C_s isomer are best envisioned as the marriage of a delocalized butadiene unit and half of a slightly distorted [8]annulene ring. As expected for delocalized π systems, the COT rings in uranocene and diuranocene have C−C bond lengths of 1.416 and 1.415 Å, respectively. Due to the complex nature of the C_s isomer and its degree of spin-contamination, multireference methods may be required for more detailed studies.

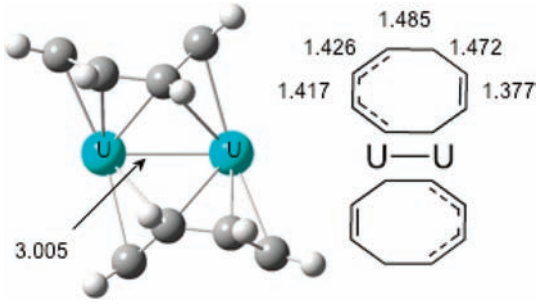

Figure 5. Perpendicular geometry for C_s $U_2(\mu$-η^6,η^4-$C_8H_8)_2$ that is 28 kJ/mol higher in energy than the coaxial isomer. Bond distances are in Ångstroms. The U−C bonds range from 2.474 to 2.748 Å, and the C−C bond values are averaged over the two rings.

In the D_{8h} isomer, the natural charge on each U, C, and H is 0.77, −0.35, and 0.25, respectively. In the C_s complex, the U charge increases to 1.04 and 1.16, indicating that 0.66 electrons from the two rings moved unequally to the U centers. The ligand to metal electron migration is also manifested in the 3.005 Å U−U bond, which is approximately a single bond as indicated by a Wiberg NPA bond order of 0.92. Such shifting of electron density reflects the drastic change in metal−ligand orbital overlap arising from rotation of the U_2 moiety. When the metals are coaxial, the uranium d and f electrons can interact with the COT ring group orbitals. After rotation, these metal-based electrons are forced to interact with the individual π electrons on the carbon atoms, resulting in the movement of electron density, elongation of the U−U bond, and distortion of the COT ring.

In the gas phase, the $U_2(C_8H_8)_2$ dimers are more stable than their separated monomers by 77.7 kJ/mol (ΔG(0 K)) for the coaxial D_{8h} isomer, $^3A_{1g}$ $U_2(\eta^8\text{-COT})_2 \rightarrow 2\ ^5B_1$ UCOT, and 49.8 kJ/mol for the perpendicular C_s isomer, $^3A'$ $U_2(C_8H_8)_2 \rightarrow 2\ ^5B_1$ UCOT. However, preparation of $U_2(COT)_2$ from two UCOT fragments is not practical because UCOT could dimerize in alternate ways (e.g., U−COT−U−COT) or could disproportionate. The disproportionation reaction $^3A_{1g}$ $U_2(\eta^8\text{-COT})_2 \rightarrow {}^3B_{2g}$ $U(\eta^8\text{-COT})_2 + {}^5A_{2u}$ U is predicted to be *endothermic* by 55.6 kJ/mol (ΔG(0 K)). Utilizing a U_2 dissociation energy of 127.6 kJ/mol,[14] the disproportionation, $2\ ^3A_{1g}$ $U_2(\eta^8\text{-COT})_2 \rightarrow 2\ ^3B_{2g}$ $U(\eta^8\text{-COT})_2 + U_2$, reaction enthalpy becomes −16.4 kJ/mol when U_2 is produced. Therefore, if $U_2(COT)_2$ can be prepared by a route not involving UCOT and if the disproportionation channel can be disabled, a whole new class of U_2 complexes becomes accessible. We are currently studying the stability of other $U_m(COT)_n$ complexes.

3.2. Protactinium and Neptunium. Both Pa_2COT_2 and Np_2COT_2 adopt D_{8h} structures similar to that of coaxial U_2COT_2 shown in Figure 1a. The key geometric parameters are presented in Table 1. Pa_2COT_2 has a singlet state with orbital occupancy $1a_{1g}{}^2 1e_{1u}{}^4$ and $\langle S^2\rangle = 0.794$; the quintet ($1a_{1g}{}^2 1e_{1u}{}^2 1e_{2g}{}^2$) is 7 kJ/mol lower and has $\langle S^2\rangle = 6.041$. Quintet Np_2COT_2 ($1a_{1g}{}^2\ 1e_{1u}{}^4 1e_{2g}{}^2 1e_{3u}{}^2$, $\langle S^2\rangle = 6.054$) is ca. 115 kJ/mol more stable than the singlet ($1a_{1g}{}^2 1e_{1u}{}^4 1e_{2g}{}^4$, $\langle S^2\rangle = 0.569$). As a consequence of the spin-unrestricted formalism, there is additional orbital mixing in both quintets, resulting in artifactual symmetry breaking. Since these systems are

(76) Brauer, D. J.; Krüger, C. *Inorg. Chem.* **1976**, *15*, 2511–2514.
(77) Cotton, F. A.; Koch, S. A.; Schultz, A. J.; Williams, J. M. *Inorg. Chem.* **1978**, *17*, 2093–2098.
(78) Bursten, B. E.; Chisholm, M. H.; Drummond, M. L.; Gallucci, J. C.; Hollandsworth, C. B. *J. Chem. Soc., Dalton Trans.* **2002**, 4077–4083.

too large to treat with CASSCF, the high symmetry D_{8h} calculations are used for further discussions. As the atomic number increases from Pa to Np, the An−An bond distances decrease from 2.54 to 2.19 Å. Although the metal to ring bond also decreases, the change is an order of magnitude smaller. The C−H bonds bend out of the ring plane toward the actinide atom by about 5°. This kind of C−H bending has been described previously.[75,79] For large rings, the carbon 2p π orbitals tip inward for maximum overlap with the metal orbitals, causing the C−H bonds to bend toward the metal. Although there are no accurate experimental atomic radii for the actinides, they were estimated by Slater to be 1.80, 1.75, and 1.75 Å for Pa, U, and Np, respectively.[80] These values are very similar because electrons are being filled into compact 5f orbitals. A recent theoretical study shows that the range of the triple-bond covalent radii of the early actinides is between 1.36 and 1.16 Å.[74] The calculated An−An distances in $Pa_2(COT)_2$, $U_2(COT)_2$, and $Np_2(COT)_2$ (2.54, 2.24, and 2.08 Å) are significantly shorter than single bonds and are closer to the length expected for triple bonds. The trend in bond lengths indicates that the actinide−actinide bond strength and bond order increases as the atomic number increases and more electrons are filled into 5f bonding orbitals. A corresponding increase in the An−An vibrational frequency (270, 349, and 354 cm^{-1}) confirms the strengthening of the An−An bond.

3.3. Thorium. In the D_{8h} Th complex, the $1a_{1g}$ orbital is higher in energy than $1e_{1u}$ orbital. However, the singlet with four electrons in the $1e_{1u}$ orbital is higher in energy than the triplet, with two unpaired electrons in the $1e_{1u}$ orbital and a pair of electrons in the $1a_{1g}$ orbital. The triplet D_{8h} complex is a second-order saddle point with two degenerate imaginary frequencies, ca. $15i$ cm^{-1} for tilting the COT rings away from the C_8 axis. The corresponding frequencies for the Pa, U, and Np complexes are all real (26, 26, and 29 cm^{-1}, respectively), indicating that these structures are stable in the coaxial configuration. By following one of the degenerate imaginary vibrational modes, the triplet $Th_2(COT)_2$ optimizes to the structure shown in Figure 1b with C_{2v} symmetry and a Th−Th−X angle of 158.4° (X is the centroid of the COT ring). The Th−Th bond length is 2.809 Å, and the distance between Th and the COT ring is 2.029 Å, in line with the trends seen for the other An_2COT_2 structures.

The HOMO of D_{8h} $Th_2(COT)_2$ corresponds to the $1e_{1u}$ 5f π-type orbital of the other diactinide metallocenes, but bending the structure lifts the original degeneracy and distorts its shape. Since the coaxial D_{8h} structure is only 2.6 kJ/mol higher than the bent C_{2v} structure, the molecule may be very floppy at room temperature. By contrast, $Pa_2(COT)_2$, $U_2(COT)_2$, and $Np_2(COT)_2$ have partially filled δ and ϕ HOMOs and are not stabilized by bending. Both coaxial and bent structures are usual for actinide complexes depending upon the competition between the ligand repulsion, bond stabilization, and electron repulsion.[81,82]

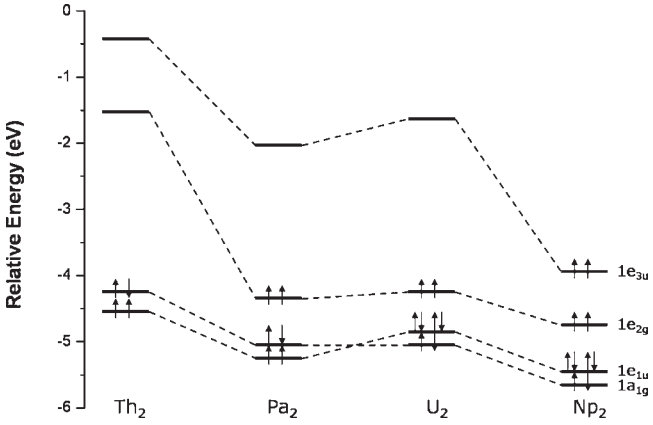

Figure 6. High spin D_{8h} $An(II)_2(COT)_2$ α frontier molecular orbital energy levels.

3.4. Orbital Analysis. The frontier molecular orbital diagram for An_2COT_2 is presented in Figure 6 using the energies of the α orbitals with significant f character from the high spin, high symmetry structures. The shapes of the orbitals of U_2COT_2 (Figure 3) are representative of the corresponding orbitals of the other An_2COT_2 complexes. As expected, the orbital energies decrease markedly as empty orbitals are populated. The $1a_{1g}$ orbital is doubly occupied for the entire series. It is higher than the $1e_{1u}$ orbital for Th and Pa but lower for U and Np. The Mulliken %f character (Table 2) of the $1a_{1g}$ orbital increases significantly from Th to Np while the %s character decreases. The $1e_{1u}$ orbital is an An−An π bonding orbital and is half filled for Th and Pa and filled for U and Np. The $1e_{2g}$ δ bonding orbital is half filled for Pa, U, and Np. Like the $1a_{1g}$ and $1e_{1u}$ orbitals, the Mulliken %f character of the $1e_{2g}$ orbital increase from Th to Np. The $1e_{3u}$ orbital is a ϕ nonbonding orbital that is empty for Th, Pa, and U, but half filled for Np. These orbital occupancies yield formal bond orders of 2, 3, 4, and 4 for Th_2COT_2, Pa_2COT_2, U_2COT_2, and Np_2COT_2, respectively. This compares well with the trend in An−An bond lengths: 2.81, 2.54, 2.24, and 2.19 Å, respectively. Adding a pair of electrons to a bonding orbital decreases the bond length by ca. 0.3 Å, while adding a pair of electrons to the nonbonding $1e_{3u}$ orbital (going from U_2COT_2 to Np_2COT_2) decreases the bond length by only 0.05 Å.

4. Conclusions

The successful synthesis of decamethyldizincocene, supported by the robust theoretical investigations of its derivatives, suggests that double-stuffed actinide metallocenes may be an interesting synthetic objective. Our studies show diuranocene is a D_{8h} coaxial minimum with a triplet ground state and a short U−U bond at the B3LYP level of theory, while the perpendicular structure is higher in energy and has distorted COT rings and a longer U−U bond. Coaxial $U_2(COT)_2$ is stable with respect to dissociation into UCOT monomers. Disproportionation of $U_2(COT)_2$ is endothermic for uranocene plus a U atom but slightly exothermic for uranocene plus $^1/_2U_2$. Similar coaxial diactinide structures have been obtained for Pa and Np, while the Th complex adopts a bent C_{2v} structure. Calculations show that as the atomic number increases, more electrons are filled into An−An 5f π- and δ-type bonding orbitals. Consequently, the An−An distance decreases from 2.81 to 2.19 Å for

(79) Brett, C. M.; Bursten, B. E. *Polyhedron* **2004**, *23*, 2993–3002.
(80) Slater, J. C. *J. Chem. Phys.* **1964**, *41*, 3199–3204.
(81) Burns, C. J.; Clark, D. L.; Sattelberger, A. P. In *Encyclopedia of Inorganic Chemistry*, 3rd ed.; King, R. B., Ed.; Wiley: Chichester, West Sussex, England, 2005.
(82) Berthet, J. C.; Thuery, P.; Ephritikhine, M. *Organometallics* **2008**, *27*, 1664–1666.

$Th_2(COT)_2$ to $Np_2(COT)_2$, respectively, and the An−An stretching frequency increases from 249 to 354 cm^{-1}. Without doubt, designing synthetic routes to complexes containing actinide−actinide bonds will require clever thinking. Hopefully, the present computational study combined with recent low-oxidation state f-element chemistry advances in the Evans group[83] will stimulate experimental endeavors to prepare this new class of diactinide complexes.

(83) Evans, W. J. *Inorg. Chem.* **2007**, *46*, 3435–3449.

Acknowledgment. The National Science Foundation (CHE-0910858) supported this research. The authors thank Drs. Charles Winter and Burt Hollandsworth for their invaluable discussion and are grateful for computer time from the Wayne State University Grid.

Supporting Information Available: Cartesian coordinates for An_2COT_2, table of energies and molecular parameters, and the full citation for refs 53 and 67. This material is available free of charge via the Internet at http://pubs.acs.org.